The *Journal of Cotton Science* 5:224-233 (2001)
http://journal.cotton.org, © The Cotton Foundation 2001

ENGINEERING & GINNING

Adaptive Signal Processing for Removal of Impulse Noise from Yield Monitor Signals

Mathew G. Pelletier *

INTERPRETIVE SUMMARY

Variability in crop yield throughout a field is well recognized. Yield monitoring is a new, rapidly evolving technique that allows harvesting equipment to measure yield instantaneously and to produce spatial yield-variability maps with the information. These yield maps make it possible to measure crop yields at any point within a field, and they provide information necessary to individually manage small sections of a field. Information from yield monitoring can form a basis for recommendations and help the grower manage inputs more effectively - such as fertilizers and other crop amendments - and optimize profitability on selected sections of a given field.

The yield monitor provides a direct means of feedback to the researcher or farmer by reporting exactly how well fields are faring in production. This information also can be used to validate variable rate applications of several inputs, such as fertilizers, insecticides, and crop amendments. Yield monitors have become commercially available for grain, cotton, potato, tomato, grape, almond, etc.

Yield monitors typically are accurate to within 5 to 10%. They output data at intervals of 20 to 100 m. Measuring mass flow in a vehicle that is moving through the field necessitates a great deal of low-pass filtering or smoothing to reduce the noise imparted from the machine to the sensors and thereby improve the yield signal. This filtering removes the short-scale field variability that is often of interest to researchers. This study examined a technique by which to improve the accuracy of the yield signal by the addition of an accelerometer, along with signal processing, for the purpose of removing unwanted impulse noise from the mass-weighing sensors used in yield monitors.

This study involved examination of adaptive digital signal processing techniques and their application in the reduction or removal of the impulse noise commonly added to yield signals when the harvester encounters holes and ditches during the harvest operation. Removal of these artifacts will improve the data obtained over a finer spatial resolution. The system demonstrated the reduction in impulse noise through the use of an accelerometer to obtain the impulse noise response. This noise response was utilized in an adaptive noise cancellation signal processing technique to reduce impulse noise in the yield signal.

ABSTRACT

The use of precision agriculture has driven the need for yield monitors. Yield monitors used for research require more rigorous standards of measurement in order to provide spatial data at a finer grid size than typically used in an on-farm application. The objective of this study was to develop a method for load-yield monitors to correct for impulse noise that occurs whenever a harvester drives over a hole, ditch, or large rocks. Removing such artifacts of the instrument will improve the quality of the data obtained over a shorter grid size, which is more appropriate for research requirements than are the typical large grid sizes of commercial yield monitors currently in use. The system developed demonstrated a reduction in impulse noise through the use of an accelerometer to obtain the impulse noise response, which was then used in an adaptive noise-cancellation signal processing technique to reduce impulse noise in the yield signal.

Variability in crop yield throughout a field is well recognized. Yield monitoring is a new, rapidly evolving technique that allows harvesting equipment to measure crop yield instantaneously and produce spatial yield variability maps with this information. These yield maps make it possible to measure crop yields at any point within a field. Yield maps provide

M.G. Pelletier, USDA-ARS, Lubbock, TX 79401. Received 30 March 2001. *Corresponding author (mpelletier@lbk.ars.usda.gov).

information necessary to individually manage small portions of the field. Information from yield monitoring can form a basis for recommendations and help the grower manage crop amendments more effectively and optimize profitability on selected sections of a given field.

The yield monitor provides direct feedback to the researcher or farmer by reporting exactly how well the fields are faring in production. This information also can be used to validate variable rate applications of several inputs, such as fertilizers, insecticides, and other crop amendments. Yield monitors have become commercially available for grain, cotton, potato, tomato, grape, almond, etc. Yield monitors have typical accuracies to within 5 to 10%, and they output data at intervals of 20 to 100 m. Recently, information gathering and treatment have been focusing on smaller areas - a typical level of management for an intensive precision farming application and data gathering operation is an area of 100 by 100 m.

With field management focused on a smaller scale, the harvester noise recorded on load-measuring devices that produce yield signals becomes more dominant. Useful signals are obtainable only when the scale is greater than 15 m. In many cases it is desirable to gather observations on a smaller scale. The overall purpose of this research was to develop a method by which to improve the short-scale accuracy of these yield monitors in mapping short-scale yield variability. The present study examined the reduction in impulse noise through use of an accelerometer to obtain the impulse noise response. This noise response then was used in an adaptive noise-cancellation signal processing technique to reduce impulse noise in the yield signal.

METHODS AND MATERIALS

This review of literature addresses the developments made in the state of the art in yield monitoring in general, and it emphasizes the currently available techniques for measuring loads on moving conveyors or belts.

Yield Measurement

Several methods have been tested over the years for the measurement of mass flow for yield monitoring. Vansichen (1993) developed a technique for measuring corn silage yield using torque transducers on the silage blower shaft and cutter-head drive shaft, and the system performed well when integrated over a 2500-kg (5512-lb) load of silage. Auernhammer et al. (1995) developed a radiometric yield-measurement system for a forage harvester that used a radioactive source and detector (not currently legal for use in the United States for food). Wild et al. (1994) reported a hay yield monitoring system for round balers with strain gages on the tongue and axle of the vehicles, which provided a measure of the weight of the baler and the bale. They also added accelerometers to measure vertical accelerations during operation and determined stationary loads within 2% of actual weight. Measurements under dynamic conditions are still under investigation.

An optical sensor has been developed by Wilkerson et al. (1994) for yield monitoring in cotton (*Gossypium hirsutum* L.). Their system used an array of lights and photo-detectors. Laboratory tests provided an integrated measurement correlation over an entire load with a coefficient of determination of $r^2 = 0.93$. Roades et al. (2000) reported on an experimental load cell-based cotton yield monitor in which the basket weight signal was integrated to provide a site-specific yield measurement. Commercial grain monitors produced by AgLeader (Ames, IA), Deere & Co. (Moline, IL), and Micro-Trak (Eagle Lake, MN) use impact plates for yield monitoring that sense the force imparted from a change in the momentum in a small quantity of grain as it hits a pressure plate.

Campbell et al. (1994) described a system for potato (*Solanum tuberosum* L.) yield monitoring. The system consisted of a single idler wheel (steel hub and rubber tire) instrumented with a single load cell. Each wheel is directly attached to a beam load cell, one on each side of the conveyor chain. The load cells measured the weight, and the integration required the addition of a speed sensor to measure the conveyor speed. The conveyor was set at a fixed angle. A similar system for measuring sugarbeet (*Beta vulgaris* L.) yield was described by Hofman et al. (1995). Calibrations of the systems were performed by correlating the output of the yield monitor to the truck weights of ≈23,000 kg (25 US ton). The weights from the yield monitor were associated with a ground position based upon

differentially corrected global satellite positioning system measurements. A correction for the harvester transport lag from digging to weighing was included through the use of a simple time delay.

Pelletier (1998) and Pelletier and Upadhyaya (1999) developed a system for yield monitoring in California tomato (*Lycopersicon esculentum* Mill.) production. In the typical tomato harvester's design, the fruit is conveyed through the machine on a series of belts and chains. The tomato harvester has only one location where fruit is not removed by either optical-mechanical color sorters or by hand. Because the goal of that research was to provide the harvester driver the total fruit weight transported to the truck, it was imperative that the measurement occurred after all fruit sorting (removal) had taken place. Thus, the final loading conveyor (boom elevator) that transports fruit into the gondolas, was the only choice for the placement of the yield monitor. At this location the boom elevator, hereafter elevator, consists of a hydraulically powered chain drive. The elevator consists of two sections: the lower section is ≈3 m (10 ft) in length and maintains an average angle of 45° with respect to the horizontal plane. The upper section of the elevator maintains an average angle of 22° with respect to the horizontal plane, but varies from -30° to +30°. Both elevators are subject to varying angles throughout the harvest operation. The design could account and correct for the changing inclination of conveyors.

Correcting for the harvester dynamics is a current research topic. Nolan et al. (1996) used a simple technique for correcting the time delay of the yield signal caused by the transport of the crop through the harvester. This harvester lag was corrected by using both a simple time-delay model and performing nearest-neighbor filtering on yield maps. Boydell (1999) reported much better results for correcting harvester lag of the yield data by deconvoluting the dynamics of the peanut harvester.

Yield Mapping

The coupling of a differentially corrected global satellite positioning system to a load monitor provides the information necessary to produce a yield map, depicting spatial location vs. crop yield for a field. Production of a useful and accurate yield map includes data-acquisition, recording, filtering, correction of harvester dynamics, and aggregation of the final data. The components for producing a yield map include a mass or volume flow sensor, a measurement of the swath width, a sensor to determine the distance traveled, and a sensor to determine the position within the field to which the yield measurements can be attributed.

The measure of crop yield is found by measuring the area traversed that corresponds to the weight of the crop harvested for that area. The harvester does not simply transport the material across the conveyor into the trucks. There is a time delay, or lag, from the point of fruit harvesting to the location of the weighing sensor. Pierce et al. (1995) reported that a simple delay model with smoothing has provided better yield maps than the more complicated maps that model the harvester dynamics as a first-order system and then perform a de-convolution of the harvester.

In the tomato harvester, there are only two very short (≈2 s) first-order sections. The first occurs at the initial point of entry into the harvester where plant stems are cut. This point is similar to a trash compactor. There is no movement of plants up the conveyor until enough plants build up behind and push them up the conveyor. The initial loading of this section takes approximately 2 s. The next section occurs directly in front of the singulation belt that presents a uniform single layer of fruit to the color sorter. This section is a 30° ramp on which fruit does not travel upward until there is enough harvested fruit behind to help push it up the ramp. The loading of this section also takes 2 s. The rest of the delay is simply accounted for by transport across the belt. The simple time-delay model followed by low-pass filtering should also apply to the tomato yield monitor, because under standard harvest operations, the belts and both first-order sections are full or almost so.

Any load sensor mounted on a moving harvester is subjected to strong harmonic vibrations from the mechanical shaker used to remove the fruit, along with additional vibration from the conveyor, engine, hydraulic motors, and random impulse inputs from the uneven surface of the field. The yield monitor should remove the effects of these noises from its signal to achieve an accurate representation of the crop mass flow as sensed by the sensor.

Three distinct cases should be considered when dealing with this noise in the signal. The first - and by far the easiest to accomplish - is removal of noise

that falls outside the frequency spectrum of interest through analog and/or digital filtering (Porat, 1997; Pelletier, 1998; and Pelletier and Upadhyaya, 1999). In the second case, the noise occurs in the frequency region of interest. Simple filtering will remove the signal of interest, so it becomes necessary to perform noise cancellation by using a sensor that has a high correlation to the noise and low correlation to the desired signal. If a suitable noise transducer with these characteristics can be developed - such as an accelerometer - then the noise can be effectively removed from the desired signal. To implement this technique, the channel through which the noise is coupling becomes crucial. If the noise channel through which the signal is transmitted remains relatively consistent through time (i.e., the transfer function doesn't vary significantly), then the noise can be removed by a matched Weiner filter (Porat, 1997). But, if the noise channel has a varying transfer function, then the noise signal can be removed only through an adaptive noise-cancellation filter (Widrow and Stearns, 1985). This research seeks to determine the suitability of either of these techniques for removal of impulse noise from the yield monitoring signal.

RESULTS

Adaptive Noise Cancellation

Input Signal and Adaptive Finite Impulse Response Filtering

In yield monitoring it is necessary to consider starting with only a single input signal from a sensor measuring the instantaneous load that is applied to the sensor. This load is subjected not only to the Earth's gravitational acceleration, but also to the accelerations present on the harvester. Assume for this theoretical case that the system is a single input system that has been digitally sampled on time interval T for n samples. This is then denoted in vector notation as detailed in Eq. 1; all vectors and matrices denoted in bold type.

$$\boldsymbol{S}(t) = [s_1, s_2, s_3,..., s_n]^T \quad [1]$$

Similarly, the weighting vector of the finite-impulse-response filter used to remove the unwanted noise can be designated by Eq. 2.

$$\boldsymbol{W}(t) = [w_1, w_2, w_3,..., w_n]^T \quad [2]$$

The scale or harvester dynamics also can be modeled by a finite-impulse-response vector (Pelletier, 1998; Pelletier Upadhyaya, 1999) designated by Eq. 3.

$$\boldsymbol{H}(t) = [h_1, h_2, h_3,..., h_n]^T \quad [3]$$

And finally, the true desired signal presented to the scale can be represented by a discrete time sampled signal, as designated by Eq. 4.

$$\boldsymbol{X}(t) = [x_1, x_2, x_3,..., x_n]^T \quad [4]$$

Theory of Adaptive Noise Cancellation

Taking for the moment a simple input and filtering operation, the output signal can be expressed in vector notation, as in Eq. 5.

$$y = \boldsymbol{X}^T\boldsymbol{W} \quad [5]$$

Next, consider the error signal as the difference between the desired response, d, and the actual response, y, as noted in Eq. 6.

$$e = d - y = d - \boldsymbol{X}^T\boldsymbol{W} = d - \boldsymbol{W}^T\boldsymbol{X} \quad [6]$$

Using the criterion function to minimize as the instantaneous mean square of the error translates into Eq. 7.

$$E\{e^2\} = E\{d^2\} - \boldsymbol{W}^T E\{\boldsymbol{X}\,\boldsymbol{X}^T\}\boldsymbol{W} - 2E\{d\,\boldsymbol{X}^T\}\boldsymbol{W} \quad [7]$$

Where $E\{\}$ is the expected value.

Next, define the input correlation matrix $\boldsymbol{R}$ and the desired cross correlation matrix $\boldsymbol{P}$, as in Eqs. 8 and 9.

$$\boldsymbol{R} = E\{\boldsymbol{X}\,\boldsymbol{X}^T\} \quad [8]$$

$$\boldsymbol{P} = E\{\boldsymbol{d}\,\boldsymbol{X}^T\} \quad [9]$$

Substituting in Eqs. 8 and 9 into Eq. 7 provides the mean-square error (MSE), as shown in Eq. 10.

$$MSE = \xi = E\{e^2\} = E\{d^2\} - \boldsymbol{W}^T\boldsymbol{R}\boldsymbol{W} - 2\boldsymbol{P}\boldsymbol{W} \quad [10]$$

Equation 10 is a quadratic function of the vector **W**.

The criterion [or objective or cost] function is minimized in the usual way: by taking the derivative of the criterion function with respect to the weights sought and setting it equal to zero, then noting that the expected value of the desired response is a constant, which leads to Eq. 11.

$$\nabla = \frac{\delta \xi}{\delta W} = 0 = 2\mathbf{R}W - 2\mathbf{P} \qquad [11]$$

Solving Eq. 11 for **W** results in a solution for the weights that will minimize the criterion function. The optimal solution weighting vector is denoted as **W*** (Eq. 12).

$$W^* = \frac{\mathbf{P}}{\mathbf{R}} \qquad [12]$$

Equation 12 - known as the Wiener-Hopf equation - provides the solution to the optimal matched filter for the noise channel as well as the foundation for adaptive noise-cancellation algorithms used to remove noise from time-varying noise channels.

Adaptive Interference Canceling of Impulse Noise

The basic noise canceling configuration is illustrated in Fig. 1 (Widrow and Stearns, 1985). However, this particular problem calls for modification of this concept in which the sensed noise passes directly into the sensor. Note, however, that the noise coupled into the signal has been subjected to an unknown filtering process or plant. The filtering process that the noise signal is subjected to is assumed to be a time-invariant linear system. In this case, an unknown finite-impulse-response filter, W*(*n*), can be used to correct the raw sensor signal to match noise coupled into the signal of interest. Through the use of adaptive system identification, an approximation finite-impulse-response filter, W(*n*), can be found for use in a stationary finite-impulse-response digital filter for noise removal. The analysis configuration for adaptive system identification is depicted in Fig. 2 (Widrow and Stearns, 1985).

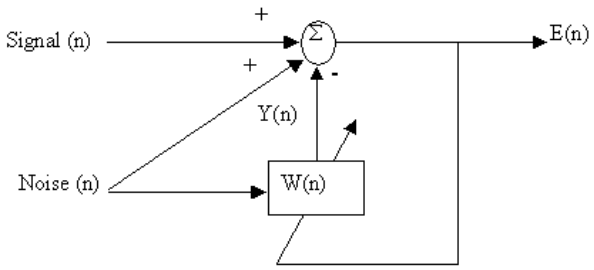

Fig. 1. An adaptive noise cancellation configuration in which, when the error is minimized, the noise has been removed from the signal.

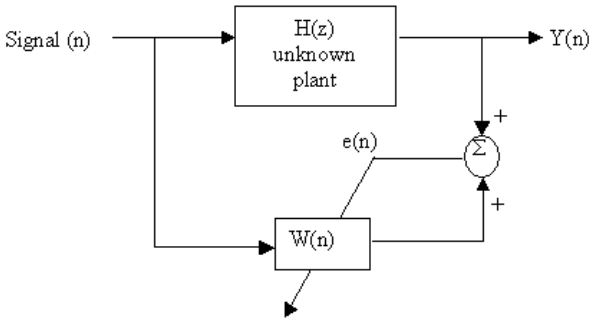

Fig 2. An adaptive system identification configuration.

Again, it should be noted that an adaptive approach is necessary only if this unknown filter is not wide-sense stationary. Formal criteria for wide-sense stationary are that two properties be satisfied: (i) the mean is the same at all time points (in this case, the gain of the filter); (ii) the covariance depends only on the time difference between time t_1 and time t_2 (as applied in this case, it denotes time-invariance and a constant frequency response of the filter).

In yield monitoring, the harvester frequently is subjected to impulse inputs that arise from the harvester's driving over irrigation ditches and holes. These impulses are filtered by the vehicle frame's chassis which functions as a spring-mass damping system. An accelerometer attached to this frame can measure this impulse input. On many yield monitors, the impulse acceleration that the accelerometer senses is altered from the impulse signal that impinges on the frame (as seen by the load sensor) due to a physical displacement or acceleration coupling between the accelerometer and the load sensor.

In the case under study, the load cell is separated from the isolated bulk container by a rubber bushing, which helped dampen the vibrations upon the load cell. The accelerometer can be coupled directly alongside the load cell, but due to the rubber bushing, the load cell has a modified load response. The bushing effectively lowers the bandwidth of the load cell and creates a lag between the accelerometer signal and the load signal as modified by an impulse input. This case also applies for belt weighing systems, because the belt effectively decouples the load from the load cell.

In both the case of the bushing and that of the belt scales, the transfer function is time-varying, as the mass in the spring mass system is the yield load. The spring in the belt weigher is the belt itself. The stiffness of the spring constant of the belt is determined by the bulk modulus of the belt and by the tension that typically varies according to the fruit loading on the belt. The spring in the bulk weigher is the rubber bushing. Regardless of the changing spring stiffness, both cases display a continuously changing mass, usually varying by a factor of 100%. From this effect alone, the resonant frequency or bandwidth of the transfer function is expected to change by the square root of $1/(M+\Delta m)$, as shown in Eq. 13, thereby changing the amount of energy that is coupled into the signal due to the impulse.

$$F_n = \sqrt{\left(\frac{k}{M+\Delta m}\right)} \qquad [13]$$

where

$\mathbf{F}_n$ = natual frequency of the spring mass system comprising the scale
k = the spring constant
m = the load, made up of the crop yield
M = the mass of the supporting structure (basket, belt, etc.)

In the simplifying case where $M = m$ (which is a fair assumption for this case), a change in the natural frequency by 0.707 is observed. The modeling will seek to determine whether a stationary Weiner filter, as quantified through adaptive system identification, would outperform an adaptive filter, given a change in the frequency response of the noise channel by a factor of 0.707. This approach could establish the framework for use of either adaptive signal processing or matched Weiner filtering in the yield monitor to remove any impulse loading.

Adaptive Noise Canceling Simulation

The model for the spring-mass simulation scale was a maximally flat second-order Butterworth (critically damped) system with a stop band frequency of 0.01 π and was implemented as a 100-point finite-impulse-response filter. This digital transfer function (filter) model of the coupling between the load cell and the accelerometer signal (used to obtain the noise signal) was used to filter the narrow-band (10-ms pulse width) impulses. The filtered impulse noise was used to model the noise as coupled into the load cell, while the unfiltered noise was used to model the noise that contains the high-frequency components, as measured by the accelerometer (Fig. 3). In all cases a small amount of Gaussian white noise was added to the model for completeness.

In Fig. 4, both the desired signal of interest and the filtered impulses are shown. The filtered impulses are the model for the impulse as measured by the load cell. This is the signal that will need to be removed from the load cell's output signal, containing both the desired signal and the filtered impulse noise (Fig. 5).

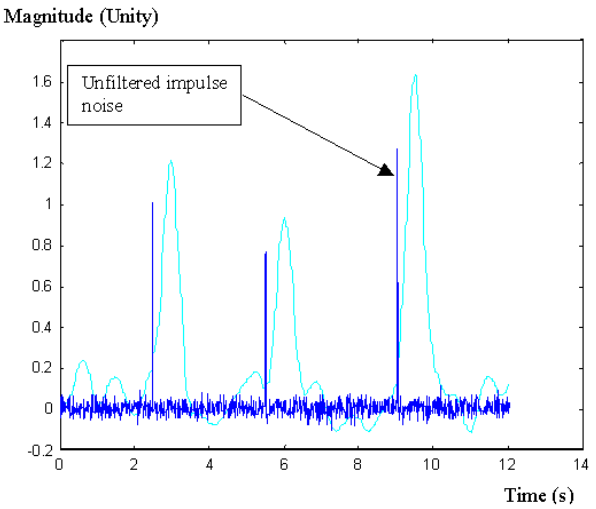

Fig. 3. Filtered impulse vs. transducer-sensed raw impulse. The sharp impulse noise (as seen by accelerometer) is used to cancel machine-filtered impulse noise (as measured by the load cell).

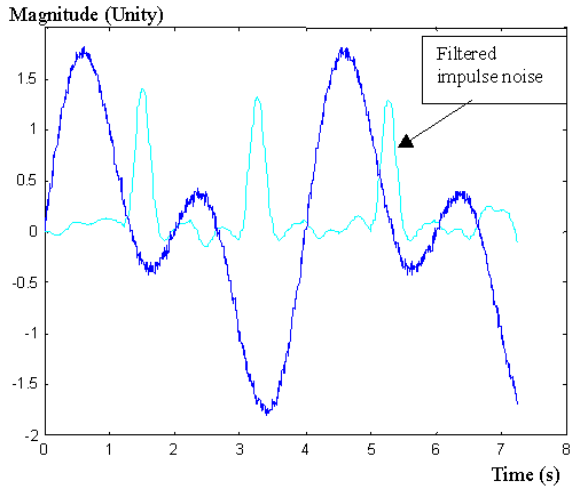

Fig. 4. The filtered impulse noise that is sensed by the load cell (cyan) vs. the true signal of interest (blue).

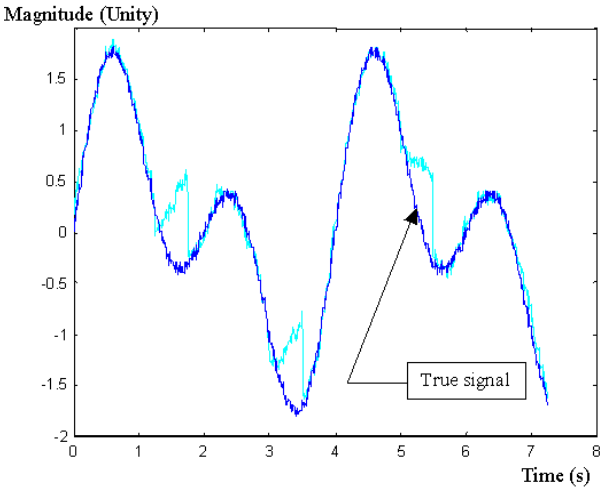

Fig. 6. The true signal of interest (blue) vs. the true signal with coupled in filtered impulse noise with reduction of the impulse noise through adaptive noise cancellation (cyan).

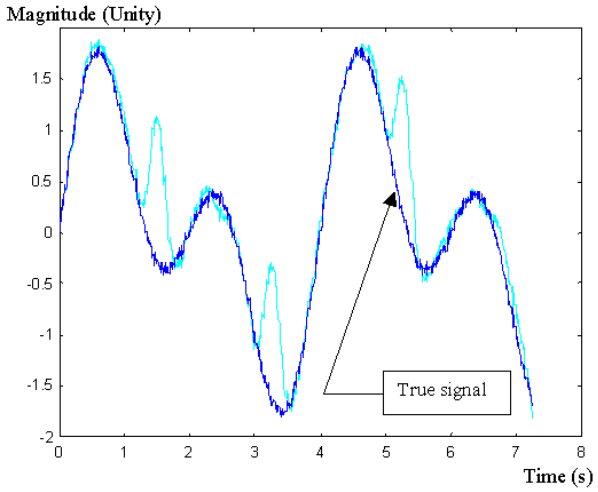

Fig. 5. The true signal of interest (blue) vs. the true signal with coupled in filtered impulse noise (cyan).

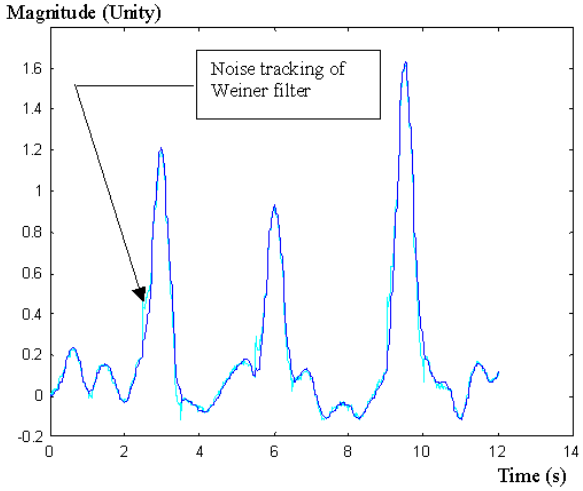

Fig. 7. The scale -filtered impulse noise (cyan) vs. the cancellation correction signal as estimated by Weiner filter from the nonfiltered machine impulse noise.

In the application of the adaptive noise cancellation algorithm, the nonfiltered impulse noise, along with the error signal, provides the feed back (Fig. 1) used to adaptively tune the weights of the filter via a real-time least-mean-square algorithm (Widrow and Stearns, 1985). The purpose of the filter is to remove the filtered impulse noise from the filtered-noise contaminated signal. The results of the adaptive filtering operation are illustrated in Fig. 6: The adaptive noise cancellation routine reduced the effect of the filtered impulses but could not converge to a point at which the entire noise signal could be removed.

The next phase examined the use of *a priori* knowledge of the impulse noise to design a stationary filter to remove the impulse noise. The technique used to design the filter involved adaptive system identification (Fig. 2). One noise pulse was used as a model in which to build a noise canceling filter. Again, the nonfiltered impulse was used as an input to the system in which to cancel the filtered impulse output at convergence.

Once the finite-impulse-response noise reduction filter had been designed, the system was checked for robustness by changing the process or plant filter by 0.707. The corner frequency was changed by this

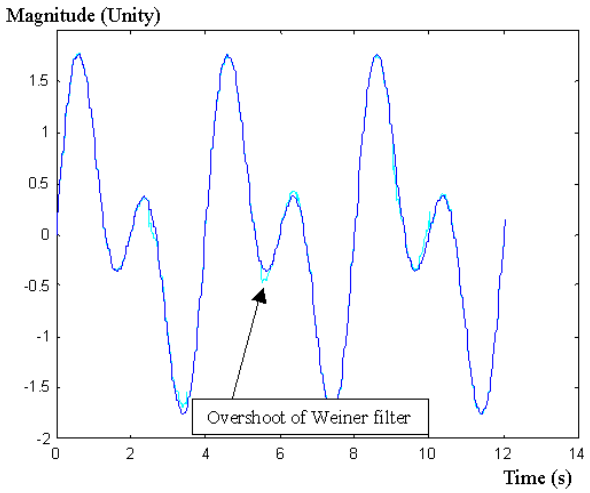

Fig. 8. The true signal (blue) vs. the estimated true signal after removal of the filtered machine noise through adaptively estimated optimal Weiner filtering that was based on the nonfiltered impulse noise (cyan).

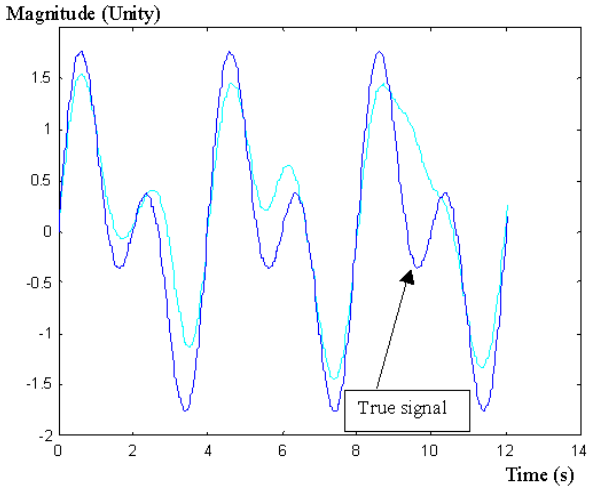

Fig. 9. A comparison of the true signal (blue) vs. the use of simple low-pass filtering technique to remove the machine-filtered impulse noise (cyan). Notice the large errors on the third set of peaks when the impulse occurs out of phase with the signal. These errors completely mask the higher frequency component of the desired signal of interest.

amount in the design of the digital low-pass filter used to model the unknown plant. The new filter then as used as the filter for the impulse to create the load cell's noise component. Figure 7 shows the comparison between this new filter acting on the noise and the noise correction signal from the estimated Weiner finite-impulse-response noise removal filter. The final output, which compares the

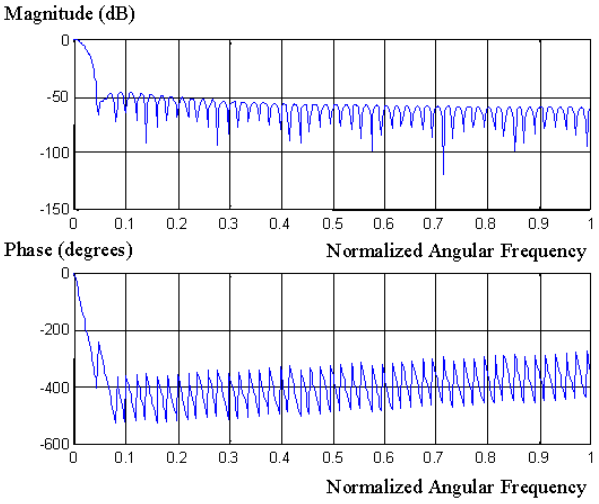

Fig. 10. The true frequency response of the model's unknown filter.

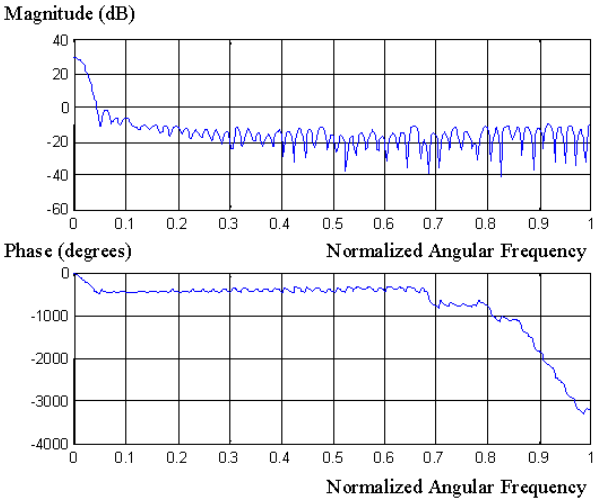

Fig. 11. The adaptive system identification estimate of the model's unknown filter.

desired signal to the output signal after filtering with the noise filter, is shown in Fig. 8. Figure 9 shows the effect of performing a simple low-pass filtering operation as an attempt to remove the filtered impulse noise from the signal.

For completeness and reference, the frequency response plots are provided: In Fig. 10, the unknown filter (plant) is given; in Fig. 11, the adaptive system identification finite-impulse-response approximation is given. Figure 12 represents the frequency response of the unfiltered impulse as would be seen by the accelerometer, and Fig. 13 shows the frequency

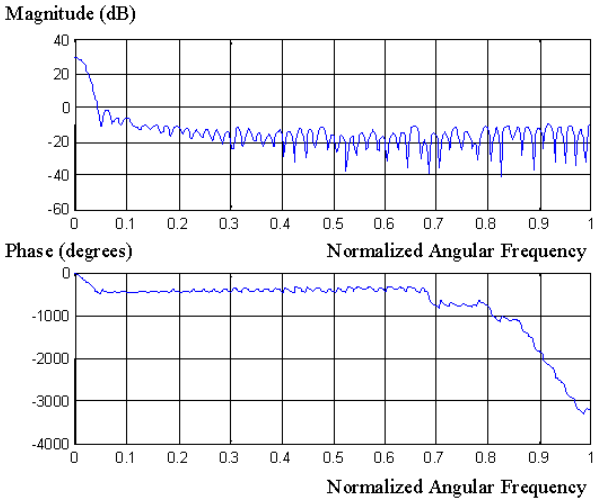

Fig. 12. The frequency response of the nonfiltered impulse noise (as measured by the accelerometer) for use in removing the filtered noise.

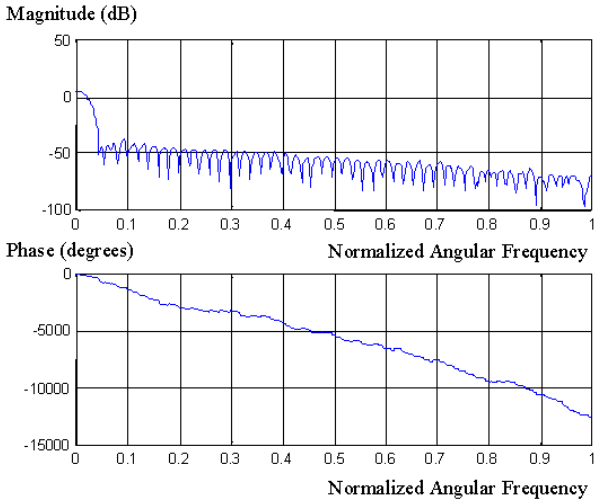

Fig. 13. The frequency response of the impulse noise as filtered by the model's unknown machine transfer function. This is the frequency response of the undesired impulse noise signal that is coupled into the load cell's yield-signal measurement.

response of the noise impulse after being filtered by the unknown plant.

SUMMARY

This research model demonstrated that a time-varying noise channel that couples impulse loading to the yield monitor's sensor can be effectively removed by both adaptive interference canceling and optimal stationary matched Weiner filtering, provided that the bandwidth of the channel stays within 0.707 times the sampled design frequency. This study also found that it was possible to obtain the optimal finite-impulse-response Weiner filter for this use by means of adaptive system identification.

The model showed that the matched filter is a better choice because it removed the impulse noise from the yield signal across the noise channel bandwidth range. The results are encouraging, and further work is under way to implement this technique as an improvement upon current signal processing removal of noise (harvester and field artifacts) from the true agronomic yield, as determined by yield monitoring.

REFERENCES

Auernhammer, H., M. Demmel, and P.J.M. Pirro. 1995. Yield measurement on a self-propelled forage harvester. ASAE Pap. 95-1757. ASAE, St. Joseph, MI.

Boydell, B. 1999. Deconvolution of site-specific yield measurements to address peanut combine dynamics. Trans. ASAE 42:1859-1865.

Campbell, R.H., S.L. Rawlins, and S. Han. 1994. Monitoring methods for potato yield mapping. ASAE Pap. 94-1584. ASAE, St. Joseph, MI.

Hofman, V., S. Panigrahi, B. Gregor, and J. Walker. 1995. In field monitoring of sugarbeets. ASAE Pap. 95-2114. ASAE, St. Joseph, MI.

Nolan, S.C., G.W. Haverland, T.W. Goddard, M. Green, and D.C. Penney. 1996. Building a yield map from geo-referenced harvest measurements. p. 885-892. *In* P.C. Robert, R.H. Rust, and W.E. Larson (ed.) Precision agriculture. ASA-CSSA-SSSA, Madison, WI.

Pelletier, M.G. 1998. Development of a tomato load/yield monitor. Ph.D. diss. Univ. of California, Davis, CA (Diss. Abstr. Int. No. pending).

Pelletier, M.G., and S.K. Upadhyaya. 1999. Development of a tomato load/yield monitor. Comput. Electron. Agric. 32:103-117.

Pierce F.J., N.W. Anderson, T.S. Colvin, J.K. Schueller, D.S. Humburg, and N.B. McLaughlin. 1995. Yield mapping. p. 211-243. *In* F.J. Pierce and E.J. Sadler (ed.) The state of site specific management for agriculture. ASA-CSSA-SSSA, Madison, WI.

Porat, B. 1997. A course in digital signal processing. John Wiley & Sons, New York, NY.

Roades, J.P., A.P. Beck, and S.W. Searcy. 2000. Cotton yield mapping: Texas experiences in 1999. *In* Proc. Beltwide Cotton Conf., San Antonio, TX. 4-8 Jan. 2000. Natl. Cotton Counc. Am., Memphis, TN.

Vansichen, R. 1993. A measurement for yield mapping of corn silage. J. Agric. Eng. Res. 55:1-10.

Widrow, B., and S.D. Stearns. 1985. Adaptive signal processing. Prentice-Hall, Englewood Cliffs, NJ.

Wild, K., H. Auernhammer, and J. Rottmeier. 1994. Automatic data acquisition on round balers. ASAE Pap. 94-1582. ASAE, St. Joseph, MI.

Wilkerson, J.B., J.S. Kirby, W.E. Hart, and A.R. Womac. 1994. Real-time cotton flow sensor. ASAE Pap. 94-1054. ASAE, St. Joseph, MI.